

**Cite this article as:** Yang Wanbo, Huo Yuanming, He Tao, et al. Microstructure Evolution of TC16 Titanium Alloy for Producing Aerospace Fasteners During Cold Compression[J]. Rare Metal Materials and Engineering, 2022, 51(02): 386-391.

ARTICLE

# Microstructure Evolution of TC16 Titanium Alloy for Producing Aerospace Fasteners During Cold Compression

Yang Wanbo<sup>1</sup>, Huo Yuanming<sup>1</sup>, He Tao<sup>1</sup>, Xue Yong<sup>2</sup>, Hu Yujia<sup>1</sup>, Shen Menglan<sup>1</sup>

<sup>1</sup> School of Mechanical and Automotive Engineering, Shanghai University of Engineering Science, Shanghai 201620, China; <sup>2</sup> School of Material Science and Engineering, North University of China, Taiyuan 030051, China.

**Abstract:** To understand the deformation mechanism and microstructure evolution of TC16 titanium alloy during cold heading, cold compression tests were conducted using a Gleeble 3800 thermo-mechanical simulator. The effects of strains (0.2, 0.4, 0.6, 0.8 and 1.0) and strain rates (0.1, 1.0 and 10.0 s<sup>-1</sup>) on the deformation behavior and microstructure evolution of the alloys were investigated. Results show that larger true strain and higher strain rate are prone to cause local grain coarsening and adiabatic shear bands within the material. True strain should be selected in the range from 0.2 to 0.6. Uniform structure and fine grains that are suitable for cold forming can be achieved at a strain rate of 1.0 s<sup>-1</sup>. The deformation softening observed during cold deformation is caused mainly by adiabatic temperature rise and local grain coarsening at larger true strains and higher strain rates.

**Key words:** TC16 titanium alloy; microstructure evolution; cold compression

TC4 (Ti-6Al-4V) alloy is an internationally recognized titanium alloy with good properties and a wide range of application. However, because of its low plasticity at room temperature<sup>[1]</sup>, hot upsetting and long time solution aging treatment are currently needed in the processing of fasteners, which results in more production steps and higher cost<sup>[2,3]</sup>. TC16 (Ti-3Al-5Mo-4.5V) titanium alloy is a type of martensite strengthening ( $\alpha + \beta$ ) titanium alloy with good mechanical and processing properties<sup>[4]</sup>, such as high plasticity, high strength, good hardenability and fatigue resistance, low sensitivity to stress, excellent weldability, machine workability, and corrosion resistance<sup>[5]</sup>. TC16 alloy has wide application in the aerospace industry<sup>[6]</sup>, in part because of its good plasticity at room temperature and excellent workability at room temperature after annealing. Fasteners can be fabricated from TC16 alloy by a cold heading process. Because of strengthening from cold deformation, the fasteners thus formed can reach the required service strength. These fasteners can also be used directly without subsequent solution aging heat treatment, so production cost is reduced, production efficiency is improved, and the production time is greatly shortened<sup>[7-10]</sup>. Therefore,

TC16 titanium alloy has received more and more attention.

The effects of cold heading on the structure and properties of TC16 titanium alloy were studied by Yang et al<sup>[11]</sup>, who proved that softening during deformation is caused mainly by adiabatic temperature rise and grain texture change. The suitability of cold heading process for production of a TC16 titanium alloy bolt was analyzed by Wang et al<sup>[12]</sup>. The bolt head was largely deformed, and the service strength required for fasteners was achieved through cold deformation. Liu et al<sup>[13]</sup> found that the grain of TC16 is fine, the distribution is uniform and  $\alpha$  phase is fully broken, which fully satisfies the microstructure requirements of titanium alloy for fasteners after cold heading. Zhang<sup>[14]</sup> researched the compression deformation of TC16 titanium alloys at room temperature and found that the dislocation density in the  $\alpha$  phase increases with increasing the deformation, and a large number of shear bands appear at larger deformation. Yang et al<sup>[15]</sup> studied the true stress-strain curves of TC16 alloy at different temperatures. The Johnson-Cook dynamic constitutive relationship of TC16 was obtained. Under quasi-static and dynamic loads, the model predictions achieve good agreement with the experimental stress-strain curve of TC16. Moiseev<sup>[16]</sup>

Received date: February 03, 2021

Foundation item: National Natural Science Foundation of China (51805314)

Corresponding author: Huo Yuanming, Professor, School of Mechanical and Automotive Engineering, Shanghai University of Engineering Science, Shanghai 201620, P. R. China., Tel: 0086-21-67791413, E-mail: yuanming.huo@sues.edu.cn

Copyright © 2022, Northwest Institute for Nonferrous Metal Research. Published by Science Press. All rights reserved.

conducted a detailed study on the phase constitution and chemical composition of TC16 alloy and found that suitable strength can be obtained for fasteners after cold working without heat treatment. Liu et al.<sup>[17]</sup> studied the effect of solution treatment on the structure and properties of TC16 titanium alloy bar, and found that after solid solution treatment, the sample contained unstable  $\beta$  phase, that the cold heading performance was poor, and that the solid solution state of TC16 titanium alloy bars was not suitable for cold heading formation. Zhuang et al.<sup>[18]</sup> studied the structural transformation of TC16 during large deformation forging through optical microscope and microhardness measurements. An adiabatic shear band was observed at the head of the nut, with greater hardness than that of the matrix. The width of the shear band increased as the heating temperature increased. The above research has contributed to the development of TC16 alloy for manufacturing fasteners. However, more research is necessary to clearly understand the cold deformation behavior of TC16 titanium alloy.

The aim of this work is to study the effects of strains and strain rates on microstructure evolution of TC16 titanium alloy during cold compression. The true stress-strain curves of TC16 titanium alloy were obtained by cold compression tests on a Gleeble-3800 thermo-mechanical simulator, and the microstructures were analyzed by scanning electron microscopy (SEM). Finally, the effects of different parameters on the deformation behavior and microstructure of TC16 titanium alloy were analyzed.

## 1 Experiment

The main chemical composition (mass fraction) of TC16 alloy includes 3.48% Al, 5.23% Mo, 4.68% V, 0.12% O, and Ti balance. Specimens were machined from an annealed wire rod ( $d=8$  mm). The material was processed by a wire-cutting machine into cylindrical samples with a diameter of 8 mm and a height of 12 mm. To investigate the metal flow behavior and microstructure evolution of TC16 during cold forming, cold compression tests were conducted on a Gleeble 3800 thermo-mechanical simulator, as shown in Fig.1. The specimens were compressed to true strains of 0.2, 0.4, 0.6, 0.8 and 1.0 at strain rates of 0.1, 1.0, and 10.0  $s^{-1}$  at room temperature. The instrument compressed the specimens along the compression direction (CD); the radial direction (RD) was perpendicular to the compression direction. After compression, the specimens were quenched by water to retain the microstructure. The true stress-strain curves were acquired by C-gauge measurements.

Compressed specimens were sectioned along the axial direction. The following steps were required to visualize the microstructure. (1) The sectioned specimens were ground using waterproof abrasive paper in grades from 240# to 1500# grit. The ground surfaces of specimens were further polished on a polishing machine with abrasive pastes of W2.5#. The sectioned surfaces of specimens were finally polished to a mirror condition. (2) The specimens were etched for 3–4 s with a solution of 2.5 mL HF+3 mL HNO<sub>3</sub>+5 mL HCL+91 mL H<sub>2</sub>O<sup>[19]</sup>. The etched surfaces were cleaned with purified water

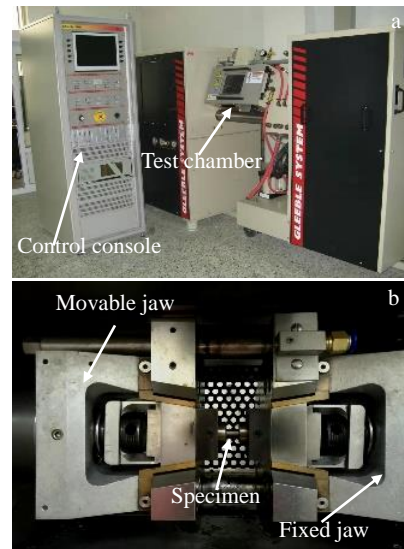


Fig.1 Gleeble-3800 thermo-mechanical materials simulator (a) and executive device of compression tests (b)

and dried with an air dryer. (3) The microstructures of specimens were observed using scanning electron microscopy (SEM). The average diameters of  $\alpha$  and  $\beta$  grains were measured using ImagePro Plus 6.0 software with the linear intercept method and a measuring multiple of 5  $\mu m$ .

## 2 Results and Discussion

Fig.2 shows the initial microstructure of a wire rod before treatment. The matrix phase consists of lath and equiaxed black  $\alpha$  phase particles with an obvious boundary and elongated white  $\beta$  phases without an obvious boundary. The sizes of the microstructures are less than 2  $\mu m$ , which indicates that the microstructure distribution is fine and uniform.

### 2.1 Effect of strain on microstructure evolution

Fig.3 shows SEM images of cold compressed specimens at true strains of 0.2, 0.4, 0.6, 0.8 and 1.0, arranged from left to right. Fig. 3a shows the initial microstructures of the undeformed specimens. The  $\alpha$  and  $\beta$  phases are evenly distributed in the alloy. At a strain of 0.2 (Fig. 3b), the microstructure is slightly deflected under the effect of compression. With an increase of deformation, the dislocation

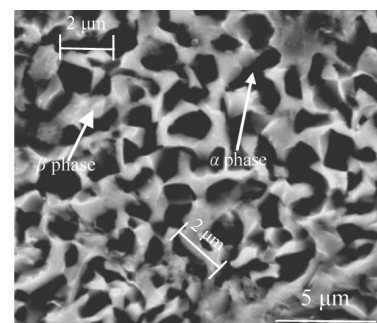


Fig.2 Initial microstructure of Ti-3Al-5Mo-4.5V wire rod

density increases, and work hardening occurs. At a strain of 0.4 (Fig. 3c), the morphology of the  $\beta$  phases changes from elongated to equiaxed, and the grain size is refined. At a strain of 0.6 (Fig. 3d), material softening is obvious. Grain coarsening occurs due to a local temperature rise and leads to nonuniform microstructure. Deformation amount should occur at a true strain of 0.6. At a strain of 0.8 (Fig. 3e), the material is further deformed, and the equiaxial structure is formed. At a strain of 1.0 (Fig. 3f), grain coarsening increases again, and an adiabatic shear band appears at a certain angle to the CD due to adiabatic temperature rise, grain slip and rotation.

The above results confirm that cold compression of TC16 titanium alloy should be conducted within the strain range between 0.2 and 0.6. Grain structure cannot be refined sufficiently when the strain is too small. When the strain is too large, the amount of deformation also increases, grain displacement and deformation become larger, the temperature rise increases, and local grain coarsening and adiabatic shear bands appear, leading to uneven microstructures<sup>[20]</sup>.

The changes in volume fraction and grain size of  $\alpha$  and  $\beta$  phases in TC16 alloy under different deformation and compression conditions were measured. The grain sizes of  $\alpha$  and  $\beta$  phases in the initial wire are almost the same, both about 2  $\mu\text{m}$ . As shown in Fig. 4a, in the original microstructure before strain occurs, the volume fraction of the  $\alpha$  phase is larger, about 52%, and the volume fraction of the  $\beta$  phase is smaller, about 48%. With an increase in strain, the volume fraction of  $\alpha$  phase gradually decreases, while that of  $\beta$  phase gradually increases. When the strain is 0.2, the volume fraction of the two phases is almost the same, both about 50%. At large strains, the volume fraction of  $\alpha$  phase decreases to a minimum of 36%, and the volume fraction of  $\beta$  phase increases to a maximum of 64%.

Fig. 4b and 4c illustrate the changes trends observed in lengths and thicknesses of grains of  $\alpha$  and  $\beta$  phases with strain. As the strain increases, the average lengths of the grains in each of the two phases have an overall tendency to increase: the maximum length of the  $\alpha$  phase and  $\beta$  phase reaches 2.5 and 3.2  $\mu\text{m}$ , respectively. The average thicknesses of the grains in each of the two phases have an overall decreasing trend: the minimum thickness of the  $\alpha$  phase and  $\beta$  phase reaches 1.2 and 1.0  $\mu\text{m}$ , respectively. However, the local

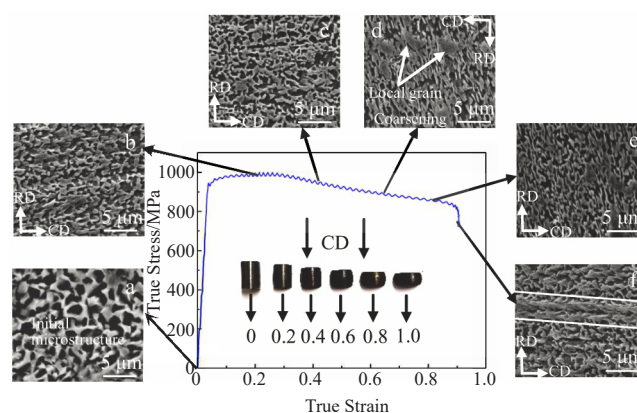


Fig.3 SEM images of cold compressed specimens at strain rate of 10.0  $\text{s}^{-1}$  and different true strains: (a) 0, (b) 0.2, (c) 0.4, (d) 0.6, (e) 0.8, and (f) 1.0

coarsening of grains and the occurrence of the adiabatic shear band phenomenon at a strain of 0.8 lead to a discrepancy in the grain size in both phases.

## 2.2 Effects of strain rates on microstructure evolution

Fig. 5 shows true stress-strain curves of cold compressed specimens at strain rates of 0.1, 1.0 and 10.0  $\text{s}^{-1}$ . The work hardening occurs as deformation begins. The dislocation density and the stress increase sharply as the strain rate increases. Plastic deformation begins at a strain of 0.05. At a strain rate of 0.1  $\text{s}^{-1}$ , the hardening increases with increasing the strain. The decline of the curves for the strain rates of 1.0 and 10.0  $\text{s}^{-1}$  indicates dynamic softening of the material. The stress-strain curve at a strain rate of 10.0  $\text{s}^{-1}$  declines faster than at 1.0  $\text{s}^{-1}$  because the softening is more pronounced at higher strain rates. As work hardening begins at a strain rate of 0.1  $\text{s}^{-1}$ , the stress-strain curve rises continuously with the increase of true strain, and the true stress reaches the maximum value of 1020 MPa at a strain of 1.0. At a strain rate of 1.0  $\text{s}^{-1}$ , the curve has little fluctuation, and the stress value is always between the curves of 0.1 and 10.0  $\text{s}^{-1}$ . The curve reaches the maximum stress of 1000 MPa at a strain rate of 10.0  $\text{s}^{-1}$  and a strain less than 0.4. At strains higher than 0.4, the curve decreases rapidly because of softening; the unloading occurs at a strain of 0.9. The three curves intersect

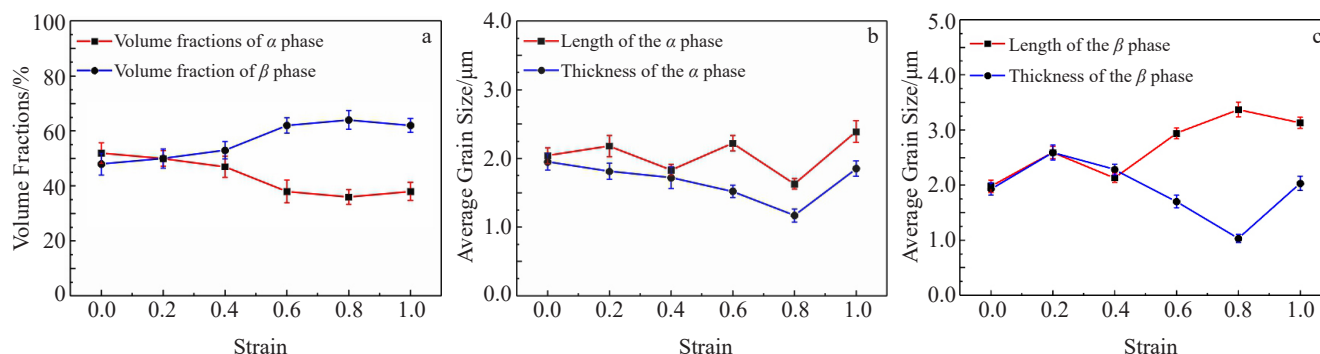


Fig.4 Changes in volume fraction (a) and grain size of  $\alpha$  (b) and  $\beta$  (c) phases with strains at strain rate of 10.0  $\text{s}^{-1}$



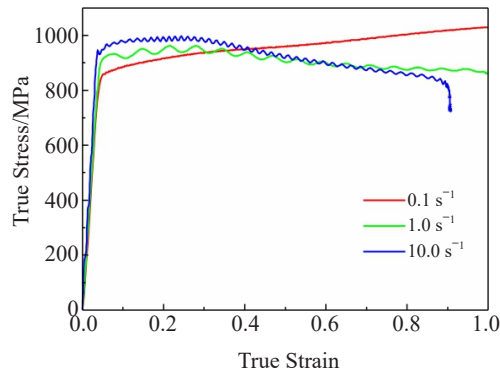


Fig.5 True stress-strain curves of cold compressed specimens at different strain rates of 0.1, 1.0 and 10.0  $s^{-1}$

at a critical strain of 0.4. When the strain is below 0.4, higher

strain rates lead to higher stress. However, when the true strain exceeds 0.4, the softening mechanism predominates, increasing material softening at higher strain rates.

In Fig. 6, SEM images of cold compressed specimens demonstrate that strain rates have a significant effect on the grain morphology of TC16 titanium alloy. At a strain rate of 0.1  $s^{-1}$ , the grain gradually changes from equiaxed to elongated along the radial direction, with a concomitant increase in deformation. At a strain rate of 1.0  $s^{-1}$ , the grain size is refined when the strain is less than 0.6, and the grain distribution is uniform. At the same strain rate, when strain is greater than 0.6, grain coarsening occurs, leading to softening of the material. At a strain rate of 10.0  $s^{-1}$ , grain coarsening occurs when the strain is 0.6. An adiabatic shear band appears at a true strain of 1.0. The true stress-strain curve at the highest strain rate declines significantly, accompanied by a noticeable softening effect.

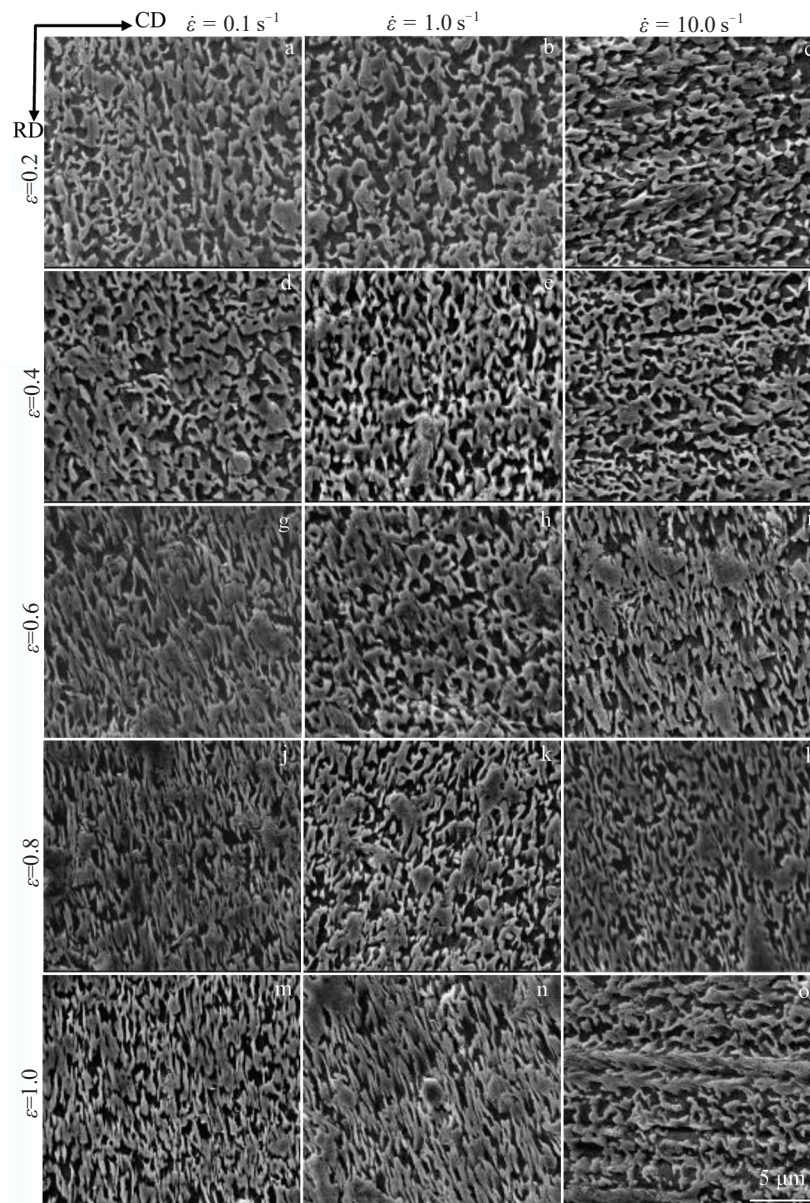


Fig.6 SEM images of cold compressed specimens under different deformation conditions

The work hardening phenomenon is obvious at the strain rate of  $0.1 \text{ s}^{-1}$ , as shown in Fig.5 and Fig.6. The strain rate of  $10.0 \text{ s}^{-1}$  is unsuitable for cold forming since this strain rate leads to obvious dynamic softening, grain coarsening, the appearance of adiabatic shear band, and a nonuniform and unstable structure. Therefore, the strain rate of  $1.0 \text{ s}^{-1}$  is preferable for cold forming, since it results in a stable microstructure with refined and uniformly distributed grain.

### 2.3 Analysis of material flow softening during cold compression

Fig. 7 shows the true stress-strain curve and strain-hardening rate at  $25^\circ\text{C}$  and strain rate of  $10.0 \text{ s}^{-1}$ . The zones in Fig. 7 are divided into regions A and B at the critical strain value ( $\varepsilon$ ) of 0.25, indicated by the vertical dotted line. In region A, the effective stress initially increases as the strain increases, and the strain hardening rate is positive. The true stress-strain curve levels off when the strain reaches a local minimum at 0.07, as indicated by the dotted circle, and the strain hardening rate curve decreases briefly at this point, and then increases briefly. As the strain continues to increase, both curves fluctuate only slightly within this region. When the material goes through the plastic yield stage, the interaction between the grains causes the grains to rotate. The shape and rotation of the grains lead to uneven deformation of the microstructure in the material, which results in fluctuation of the curves<sup>[21]</sup>.

In region B, the effective stress decreases as the strain increases. The strain hardening rate fluctuates only slightly until it drops off steeply at the highest strains. These results indicate the occurrence of material flow softening of the TC16 wire rod in region B of Fig.7.

Fig.8 shows SEM images of cold compressed specimens at a true strain of 1.0 and strain rates of  $1.0$  and  $10.0 \text{ s}^{-1}$ . Fig.8a reveals that at a strain rate of  $1.0 \text{ s}^{-1}$ , the grains are almost perpendicular to the compression direction and elongated along the radial direction. The excessive heat of deformation at higher strains causes a transformation of some areas of the lamellar structure into local grain coarsening, which results in a nonuniform structure. At higher strain rates, the deformation time of the material is shortened, the change in the microstructure cannot be completed, and the deformation energy is higher, which results in the formation of adiabatic shear bands, as shown in Fig.8b. The angle of inclination of the adiabatic shear band to the compression direction is determined by the strength of the shearing force.

Compared with the close-packed hexagonal  $\alpha$  phases, the body-centered cubic  $\beta$  phases have more slip systems. The low plasticity of the  $\beta$  phase relative to the  $\alpha$  phase renders that it is more prone to deformation. The softening phenomenon occurring at higher strain rates during cold deformation is caused mainly by adiabatic temperature rise and local grain coarsening structure.

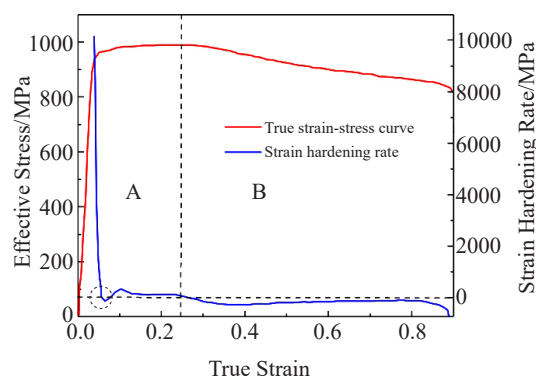


Fig.7 True stress-strain curve and strain-hardening rate at  $25^\circ\text{C}$  and strain rate of  $10.0 \text{ s}^{-1}$

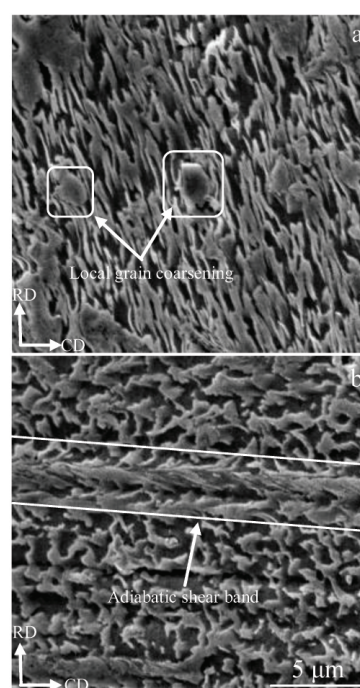


Fig.8 SEM images of cold compressed specimens at true strain of 1.0 and different strain rates: (a)  $1.0 \text{ s}^{-1}$  and (b)  $10.0 \text{ s}^{-1}$

### 3 Conclusions

1) The cold compression deformation of TC16 titanium alloy should be performed in the strain range between 0.2 and 0.6 at a strain rate of  $10 \text{ s}^{-1}$ . The grain cannot be refined sufficiently when the strain is too small. When the strain is too large with higher strain rates, local grain coarsening and adiabatic shear band appear easily, leading to uneven microstructures.

2) The lengths of the  $\alpha$  and  $\beta$  phases increase and the thicknesses decrease with increasing the strain. At a lower strain rate of  $0.1 \text{ s}^{-1}$ , work hardening is stable with the increase of strain. At a higher strain rate of  $10.0 \text{ s}^{-1}$ , microstructure uniformity is destroyed by a local temperature rise. A strain rate of  $1.0 \text{ s}^{-1}$  should be selected which is most suitable for



cold forming of TC16 titanium alloy.

## References

- Wang L D, Liu F L, Zhao Q Y et al. *Hot Working Technology*[J], 2015, 44(13): 150
- Hou F Q, Hu B, Sun X P et al. *Titanium Industry Progress*[J], 2017, 34(5): 18
- Wu C Z. *Aerospace Materials & Technology*[J], 2007, 37(3): 61
- Shen M L, Huo Y M, He T et al. *Materials Today Communications*[J], 2020, 24: 101 053
- Liu Q M, Zhang C, Liu S F et al. *Journal of Sichuan University, Natural Science Edition*[J], 2015, 52(2): 377
- Li M Q, Li H F, Xiong A M et al. *Forging & Stamping Technology*[J], 2018, 43(7): 96
- Sha A X, Wang Q R, Li X W. *Rare Metal Materials and Engineering*[J], 2006, 35(3): 455 (in Chinese)
- Li X W, Sha A X, Su S M et al. *Twelfth Annual Conference on Materials Science and Alloy Processing of Chinese Society of Nonferrous Metals*[C]. Zhangjiajie: The Nonferrous Metals Society of China, 2007: 74 (in Chinese)
- Wu C Z, Li X W. *Titanium Industry Progress*[J], 2006, 23: 17 (in Chinese)
- Wu C Z, Li X W. *Thirteenth National Symposium on Titanium and Titanium Alloys*[C]. Luoyang: The Nonferrous Metals Society of China, 2008: 580 (in Chinese)
- Yang Y, Dong L M, Guan S X et al. *Transactions of Nonferrous Metals Society of China*[J], 2010, 20: 107
- Wang F Q, Sha C P, Sun X L. *Journal of Materials and Metallurgy*[J], 2013, 12: 218
- Liu Q M, Zhang C H, Liu S F et al. *Hot Working Technology*[J], 2014, 43(4): 17
- Zhang Z Q. *Thesis for Doctorate*[D]. Beijing: University of Chinese Academy of Sciences, 2011 (in Chinese)
- Yang Y, Ceng Y, Wang B F. *Transactions of Nonferrous Metals Society of China*[J], 2007(S1): 466
- Moiseev V N. *Metal Science and Heat Treatment*[J], 2001, 43(1): 73
- Liu Q M, Zhang Z H, Yang H Y et al. *Advanced Materials Research*[J], 2014, 2951(1764): 1588
- Zhuang B T, Liu F L, Huang H. *Advanced Materials Research* [J], 2014, 3381(2009): 1331
- Wang B F, Yang Y. *Materials Science and Engineering A*[J], 2008, 473(1): 306
- Tang X, Bai Q, Huo Y M et al. *Indian Journal of Engineering and Materials Sciences*[J], 2017, 24(6): 447
- Chen S D, Lu R H, Jian S et al. *Materials Science and Technology*[J], 2018, 26(4): 88

## 航空航天紧固件用 TC16 钛合金在冷压缩过程中的组织演变

杨万博<sup>1</sup>, 霍元明<sup>1</sup>, 何 涛<sup>1</sup>, 薛 勇<sup>2</sup>, 胡玉佳<sup>1</sup>, 沈梦蓝<sup>1</sup>

(1. 上海工程技术大学 机械与汽车工程学院, 上海 201620)

(2. 中北大学 材料科学与工程学院, 山西 太原 030051)

**摘 要:** 为了解钛合金在冷压缩过程中的变形机理和微观组织演变, 使用 Gleeble 3800 热模拟试验机进行冷压缩试验。在冷压缩试验中, 通过不同应变 (0.2、0.4、0.6、0.8 和 1.0) 和不同应变率 (0.1、1.0 和 10.0 s<sup>-1</sup>), 来研究应变和应变率对钛合金冷变形中微观组织演变的影响。结果表明, 较大的真应变和较高的应变率容易使材料内部产生局部晶粒粗化和绝热剪切带。真应变应选择在 0.2~0.6 的范围内。1.0 s<sup>-1</sup> 的应变速率下, 组织均匀且晶粒细小, 适合冷变形。在冷变形过程中观察到的变形软化主要是由在较大的真应变和应变速率下产生的绝热温升和局部晶粒粗化引起的。

**关键词:** TC16 钛合金; 微观组织演变; 冷压缩变形

**作者简介:** 杨万博, 男, 1996 年生, 硕士, 上海工程技术大学机械与汽车工程学院, 上海 201620, E-mail: 17862976062@163.com